Original Investigation

Identifying Large-Scale Brain Networks in Fragile X Syndrome

Scott S. Hall, PhD; Heidi Jiang, BS; Allan L. Reiss, MD; Michael D. Greicius, MD

IMPORTANCE Fragile X syndrome (FXS) is an X-linked neurogenetic disorder characterized by a cognitive and behavioral phenotype resembling features of autism spectrum disorder. Until now, research has focused largely on identifying regional differences in brain structure and function between individuals with FXS and various control groups. Very little is known about the large-scale brain networks that may underlie the cognitive and behavioral symptoms of FXS.

OBJECTIVE To identify large-scale, resting-state networks in FXS that differ from control individuals matched on age, IQ, and severity of behavioral and cognitive symptoms.

DESIGN, SETTING, AND PARTICIPANTS Cross-sectional, in vivo neuroimaging study conducted in an academic medical center. Participants (aged 10-23 years) included 17 males and females with FXS and 16 males and females serving as controls.

MAIN OUTCOMES AND MEASURES Univariate voxel-based morphometric analyses, fractional amplitude of low-frequency fluctuations (fALFF) analysis, and group-independent component analysis with dual regression.

RESULTS Patients with FXS showed decreased functional connectivity in the salience, precuneus, left executive control, language, and visuospatial networks compared with controls. Decreased fALFF in the bilateral insular, precuneus, and anterior cingulate cortices also was found in patients with FXS compared with control participants. Furthermore, fALFF in the left insular cortex was significantly positively correlated with IQ in patients with FXS. Decreased gray matter density, resting-state connectivity, and fALFF converged in the left insular cortex in patients with FXS.

CONCLUSIONS AND RELEVANCE Fragile X syndrome results in widespread reductions in functional connectivity across multiple cognitive and affective brain networks. Converging structural and functional abnormalities in the left insular cortex, a region also implicated in individuals diagnosed with autism spectrum disorder, suggests that insula integrity and connectivity may be compromised in FXS. This method could prove useful in establishing an imaging biomarker for FXS.

JAMA Psychiatry. doi:10.1001/jamapsychiatry.2013.247
Published online September 25, 2013.

Supplemental content at jamapsychiatry.com

Author Affiliations: Center for Interdisciplinary Brain Sciences Research, Department of Psychiatry and Behavioral Sciences, Stanford University School of Medicine, Stanford, California (Hall, Reiss); Functional Imaging in Neuropsychiatric Disorders Lab, Department of Neurology and Neurological Sciences, Stanford University School of Medicine, Stanford, California (Jiang, Greicius); currently a graduate student in the Northwestern University Interdepartmental Neuroscience Program, Feinberg School of Medicine, Northwestern University, Chicago, Illinois (Jiang); Departments of Radiology and Pediatrics, Department of Neurology and Neurological Sciences, Stanford University School of Medicine, Stanford, California (Reiss).

Corresponding Author: Scott S. Hall, PhD, Center for Interdisciplinary Brain Sciences Research, Department of Psychiatry and Behavioral Sciences, Room 1365, Stanford University, 401 Quarry Rd, Stanford, CA 94305 (hallss@stanford.edu).

During the past decade, investigators conducting systems neuroscience research have identified several large-scale brain networks that are coactive during periods when an individual is at rest (ie, not engaged in a specific ongoing cognitive activity).[1] Dissociable resting-state networks include, among others, the default-mode network, the executive control network, the salience network, and the visual, sensorimotor, and language networks.[2] These networks have now been reliability identified in neurotypical individuals as well as in those diagnosed with various neuropsychiatric conditions,[3-5] including individuals with autism spectrum disorder (ASD).[6-8] Increasing evidence, for example, suggests that in high-functioning individuals with ASD, both intranetwork and internetwork connectivity may be decreased compared with controls.[7,9]

A significant issue for investigators attempting to replicate findings in study samples of individuals with ASD concerns the inevitable neurobiological heterogeneity of the disorder itself.[10] This is because ASD is diagnosed on the basis of lists of specific behavioral inclusion and exclusion criteria contained in the *DSM-IV* or *DSM-5*, which themselves are subject to refinement and revision.[11] A solution to this problem is to study individuals in whom the underlying biological cause is known but whose behavioral phenotype appears to overlap substantially with ASD. A particularly good example of such a phenocopy disorder is fragile X syndrome (FXS),[12] the most common known form of inherited intellectual disability. Individuals with FXS display several behaviors that, on the surface, appear similar to those with ASD, including eye gaze avoidance, hyperactivity, increased anxiety, and stereotypical behaviors, as well as mild to moder-

ate intellectual deficits in visuospatial skills, executive functioning, language, mathematics, memory, and attention.[13-15] Investigation into the large-scale brain networks underlying FXS may provide important clues toward identifying new treatments for FXS and may provide a window into an increased understanding of the pathogenesis of ASD (or at least the mechanisms underlying ASD-like behaviors).[11]

In FXS, mutations to a single gene (*FMR1*; GenBank accession No. L19476-L19493) at locus 27.3 on the long arm of the X chromosome produce excessive methylation and transcriptional silencing of *FMR1*,[16] resulting in reduced production or absence of the fragile X mental retardation protein (FMRP), a key protein involved in synaptic plasticity and dendritic maturation in the brain.[17] Neuroimaging studies[18,19] have shown region-specific alterations in brain structure in children and adolescents with FXS, including enlargement of the caudate nucleus and hippocampus and diminution of the superior temporal gyrus, cerebellar vermis, amygdala, and insular cortex, among other regions.[20] Differential regional brain growth in FXS is thought to be a consequence of aberrant synaptic pruning and dendritic maturation in the prenatal and/or postnatal periods associated with deficient or absent FMRP.[19,20] Studies[20] investigating the neural basis of cognitive deficits in patients with FXS also have shown abnormal activation of the insula, caudate, and hippocampus when individuals with FXS are engaged in cognitive tasks involving eye gaze processing, working memory, executive function, and behavioral inhibition.

To our knowledge, no studies have investigated the large-scale brain networks (ie, neural systems that are distributed across the entire brain) that may underlie some of the cognitive and behavioral symptoms of FXS. Although resting-state connectivity studies can provide important information pertaining to the degree of intranetwork and internetwork connectivity in the resting brain, the extent to which the amplitude of spontaneous activity of a region within a network may be abnormal cannot be evaluated using this approach alone. Recently, however, a new method to quantify the amplitude of brain activity within regions of a network—fractional amplitude of low-frequency fluctuations (fALFF)—has been proposed.[21] This new method, in combination with traditional resting-state functional magnetic resonance imaging (fMRI), was used in the present study for the first time in a homogeneous genetic disorder with autistic-like symptoms. This study therefore extends previous findings in several ways: (1) we identified the potential large-scale resting-state networks underlying the cognitive and behavioral features of individuals diagnosed with FXS, (2) we measured the amplitude of brain activity within each network by using fALFF to identify the extent to which regional spontaneous activity may be abnormal in FXS, and (3) we examined the convergence between region-specific differences in gray matter density, fALFF, and network connectivity to identify convergent regions of abnormality in FXS.

Methods

Participants

Participants with FXS were recruited via an e-mail sent to members of the National Fragile X Foundation and from an ongoing longitudinal study of children and adolescents with FXS conducted at Stanford University. Participants to serve as controls were recruited via community media and state-run agencies for individuals with developmental disabilities in the local area (eg, Regional Centers). Individuals in the FXS group were included if they were aged between 10 and 23 years, had an IQ between 50 and 90 points on the Wechsler Abbreviated Scale of Intelligence,[22] and could demonstrate that they were able to remain motionless for 10 minutes while lying in the supine position with eyes closed in a mock scanner. During ongoing recruitment of participants with FXS, we recruited control participants who matched the individuals with FXS in terms of age (±3 years), IQ (±10 points), and severity of autistic symptoms (±5 points on the Social Communication Questionnaire [SCQ]).[23] We also attempted to match individuals on severity of behavioral problems using the Aberrant Behavior Checklist-Community (ABC-C).[24] Individuals in both groups were excluded from the study if they were born preterm (<34 weeks), had low birth weight (<2000 g), showed evidence of a genetic condition other than FXS, exhibited sensory impairments, or had any serious medical or neurologic condition that affected growth or development (eg, seizure disorder, diabetes mellitus, and congenital heart disease). Finally, individuals were excluded if their body contained materials that would preclude an MRI scan (eg, dental braces). Control participants were subsequently screened for FXS to confirm that they did not have the disorder. All protocols were approved by the human subjects committee at Stanford University School of Medicine, and all parents gave consent for their child to participate in the study. Forty individuals (20 with FXS, 20 controls) met the study inclusion criteria, but scans for 3 participants in the FXS group and 4 controls were later discarded because of excessive movement (see below). The final sample therefore consisted of 17 participants with FXS (8 males, 9 females) and 16 matched control participants (12 males, 4 females). All participants with FXS had a confirmed genetic diagnosis of FXS (ie, >200 CGG repeats on the *FMR1* gene and evidence of aberrant methylation) as evidenced by standard Southern blot techniques. Two male participants with FXS were mosaic (ie, an additional unmethylated fragment was detected in the premutation range). Five control participants had a comorbid diagnosis (2 had attention-deficit/hyperactivity disorder; 1, posttraumatic stress disorder; and 2, ASD). As reported in the **Table**, the 2 groups did not differ significantly in age, IQ, autistic symptoms, and severity of behavioral problems.

Three participants (18%) in the FXS group and 5 participants (31%) in the control group obtained scores on the SCQ that were considered to be in the ASD range (ie, ≥15 points). Nine participants (53%) with FXS and 4 controls (25%) had been taking psychoactive medications for at least 1 month prior to the study. Given that FXS is an X-linked disorder and that there are well-known differences in clinical presentation between males and females with the disorder, we examined whether there were potential sex differences within the FXS group on the measures. As expected, mean (SD) IQs were significantly higher in females with FXS (73.0 [8.0]) than in males with FXS (59.8 [9.0]; $t_{15} = 3.21$; $P = .006$). There were no other significant differences between female and male participants with FXS in the measures. In both groups, scores on the SCQ and ABC-C were sig-

Table. Demographic Characteristics

Characteristic	FXS Group	Control Group	*P* Value
Sex, No.			
Male	8	12	.10
Female	9	4	
Age, mean (SD), y	17.52 (4.68)	16.31 (4.06)	.44
WASI standard score, mean (SD)	66.76 (10.67)	63.81 (11.53)	.45
SCQ score, mean (SD)			
Reciprocal social interaction	2.94 (3.41)	2.69 (2.84)	.82
Communication domain	4.59 (2.52)	5.81 (2.88)	.20
Restricted, repetitive, and stereotyped patterns of behavior domain	1.76 (1.30)	2.63 (2.60)	.24
Total	9.59 (6.52)	11.62 (7.47)	.42
ABC-C score, mean (SD)			
Irritability, agitation, crying subscale	4.47 (5.56)	5.56 (6.04)	.58
Lethargy/social withdrawal subscale	7.11 (7.38)	6.56 (9.06)	.85
Stereotypic behavior subscale	1.24 (1.71)	2.94 (4.14)	.13
Hyperactivity/noncompliance subscale	5.29 (4.65)	8.06 (6.87)	.18
Inappropriate speech subscale	2.59 (2.47)	2.06 (2.29)	.53
Total	20.82 (18.03)	25.13 (23.33)	.56

Abbreviations: ABC-C, Aberrant Behavior Checklist–Community; FXS, fragile X syndrome; SCQ, Social Communication Questionnaire; WASI, Wechsler Abbreviated Scale of Intelligence.

nificantly correlated (FXS, $r_{17} = 0.61$; $P < .01$ vs controls, $r_{16} = 0.79$; $P < .001$). Age and IQ were not associated with scores on the SCQ and ABC-C in either group.

Data Acquisition

Participants received a 4-minute 33-second structural scan followed by an 8-minute resting-state scan. During the structural scan, the individuals were instructed to remain as still as possible while they watched a video of their choosing. During the resting-state scan, participants were instructed to remain awake and as still as possible with their eyes closed. Magnetic resonance imaging was performed on a 3.0-T whole-body scanner (GE Discovery MR750; GE Healthcare Systems). High-resolution structural scans were acquired using a spoiled gradient-recalled acquisition in the steady-state sequence (124 slices; 0.86-mm^2 in-plane and 1.5-mm through-plane resolution; flip angle, 15°; field of view, 22 cm), facilitating subsequent localization and coregistration of functional data. A T2*-sensitive gradient-echo spiral-in/out pulse sequence[25] was used for functional imaging (repetition time, 2000 milliseconds; echo time, 30 milliseconds; flip angle, 80°; matrix, 64 × 64 pixels; field of view, 22 cm). Thirty oblique axial slices were obtained parallel to the anterior/posterior commissure with a 4-mm slice thickness and 1-mm skip. A high-order shimming procedure was used to reduce B0 heterogeneity before the functional scan.[26] Cardiac and respiratory processes were monitored using the scanner's built-in photoplethysmograph placed on a finger of the left hand and a pneumatic belt strapped around the upper abdomen, respectively. Cardiac and respiratory data were sampled at 40 Hz. A file containing cardiac trigger times and respiratory waveforms was generated for each scan by the scanner's software.

Data Analysis

Voxel-Based Morphometry

All collected T1 images were used for anatomic analyses, which were carried out using FSL-VBM[27] (http://fsl.fmrib.ox.ac.uk/fsl/fslwiki/fslvbm/userguide), a voxel-based morphometry-style analysis.[28,29] Anatomic images were extracted using the Oxford Centre for Functional MRI of the Brain's (FMRIB's) brain-extraction tool,[30] with brain masking performed semiautomatically to ensure proper extraction. Tissue-type segmentation was performed using FMRIB's automated segmentation tool (FAST; expectation-maximization algorithm) with spatial intensity inhomogeneity correction.[31] Segmented gray matter maps were subsequently used in functional analyses as voxelwise regressors to correct for any differences in gray matter density across groups. Segmented gray-matter partial-density images were then aligned to Montreal Neurological Institute 152 standard space using affine registration[32] and nonlinear registration using FMRIB's nonlinear image restoration tool.[33] To compare gray matter density across groups, individual gray matter maps were averaged to create a study-specific template, to which the native gray matter images were then nonlinearly reregistered. The registered partial density images were then modulated (to correct for local expansion or contraction) by dividing by the Jacobian of the warp field. The modulated segmented images were finally smoothed with an isotropic full-width half-maximum gaussian kernel with a sigma of 3 mm. We performed manual quality control and inspection of the processing steps and outputs and did not have to correct the results of classification. To perform significance testing between patients with FXS and controls, a voxelwise general linear model was applied with permutation-based nonparametric testing, using threshold-free cluster enhancement (TFCE) as implemented in FSL[34] and $q < 0.05$ false discovery rate (FDR) corrected.

Preprocessing: Resting-State fMRI

Images were preprocessed and analyzed using FMRIB's Software Library (FSL, version 4.1).[27] The first 6 of 240 volumes were discarded to allow for signal stabilization, and the following preprocessing steps were applied: motion correction using least-squares minimization,[32] removal of nonbrain structures,[30] re-

sampling to 2 mm and spatial smoothing with a 6-mm full-width half-maximum gaussian kernel, mean-based intensity normalization of all volumes by the same factor, high-pass filtering with a gaussian-weighted least-squares straight-line fitting (σ, 75 seconds), and gaussian low-pass filtering (σ, 2.8 seconds). For the fALFF analysis described below, data were not band passed, but all other steps were identical. Following alignment to each participant's high-resolution T1-weighted image, functional scans were registered to the MNI152 standard space using affine linear registration.[32] Several sources of noise were subsequently regressed out of the 4-dimensional images, including variance from cerebrospinal fluid, white matter, global signal, and the 6 standard movement parameters.

Resting-state scans from 17 patients with FXS and 16 matched-symptom controls were retained after 3 FXS scans and 4 matched control scans were discarded (mean displacement exceeded 1 mm or maximum translation or rotation exceeded 3 mm or 3°, respectively). Physiologic signals were monitored and recorded during the resting-state scan for all participants except one with FXS, but these signals were not regressed out of the 4-dimensional images because several individuals had poor data recordings. Mean heart rate did not differ significantly in the data that were retained (11 individuals with FXS: mean, 79.27 [16.25] beats/min vs 14 controls: mean, 75.29 [9.78] beats/min; $P = .45$). Mean respiration rate also did not differ significantly in the data that were retained (14 FXS: mean, 20.43 [3.03] breaths/min vs 16 controls: mean, 19.5 [4.26] breaths/min; $P = .51$).

Fractional Amplitude of Low-Frequency Fluctuations

The fALFF analysis was performed using the resting-state fMRI data analysis toolkit (REST, version 1.6).[35] As described above, 4-dimensional data did not undergo band-pass filtering for this particular analysis. First, the time series for each voxel was transformed to the frequency domain, and the square root of power at each frequency was calculated to derive an amplitude spectrum.[21] The sum of amplitudes across a chosen frequency range (ie, 0.01-0.10 Hz) then was divided by the sum of amplitudes across the entire frequency range (0-0.25 Hz). Subsequently, each fALFF value per voxel was divided by the mean fALFF value across the brain to yield normalized fALFF maps. Among patients with FXS, age, IQ, and SCQ scores also were used in a separate analysis as covariates of interest to identify regions where age, IQ, and SCQ scores varied with fALFF values. Gray matter partial-volume maps were included as voxelwise nuisance regressors in between-group as well as within-group covariate comparisons. A voxelwise general linear model was applied using permutation-based nonparametric testing for group-level analyses using TFCE with $q < 0.05$ FDR correction for between-group comparisons and TFCE with $P < .001$ uncorrected for within-group covariate analyses.

Group-Independent Component Analysis and Dual Regression

The dual-regression technique was used to measure connectivity within multiple networks identified by independent component analysis.[36] Group-independent component analysis was performed to extract population-specific spatial maps showing large-scale connectivity patterns. The concatenated data set was decomposed into 30 independent components, and by visual inspection, 11 components corresponding to large-scale brain networks were identified. Dual regression was then performed: the 11 components were fed into a spatial regression against each of the 33 original single-subject data sets, and resulting time courses were regressed against each participant's 4-dimensional data to estimate subject-specific network spatial maps. For group analyses, voxelwise nonparametric permutation testing was applied to these subject-specific spatial maps.[37] Gray matter partial-volume maps were included as voxelwise nuisance regressors in between-group comparisons.[38] Between-group difference maps were masked with combined-group, 1-sample maps derived from all 33 participants, thresholded at $q < 0.01$ and FDR corrected so that any detected differences were within the network of interest.

Results

Differences in Gray Matter Density Between FXS and Control Groups

Voxel-based morphometry as implemented by FSL was used to assess differences in gray matter density between groups. Results showed that patients with FXS had increased gray matter density in the bilateral caudate head, left hippocampus, left planum temporale, left angular gyrus, and left superior parietal lobule compared with controls. Patients with FXS also had decreased gray matter density in the bilateral insular cortex, precuneus cortex, thalamus, and subgenual cingulate cortex, among other areas compared with controls (**Figure 1** and Supplement [eTable 1]).

Differences in Fractional Amplitude Between FXS and Control Groups

We used the fALFF method to measure the ratio of low-frequency amplitude (0.01-0.10 Hz) to the entire spectrum.[21] Using TFCE with a $q < 0.05$ FDR correction, we found that patients with FXS showed significantly decreased fractional amplitude in the 0.01- to 0.10-Hz frequency range in multiple regions compared with controls, including the bilateral insular cortex, precuneus cortex, and anterior cingulate cortex (**Figure 2**A and the Supplement [eTable 2]). For the opposite comparison, patients with FXS displayed greater fALFF in the bilateral caudate head, subgenual cingulate cortex, and bilateral amygdala among other areas, but this finding did not survive correction for multiple comparisons (TFCE, $P < .005$ uncorrected, not displayed).

Subsequently, voxelwise fALFF for all patients with FXS was covaried with age, IQ, and SCQ total scores. A cluster in the left insular cortex was significantly positively correlated with IQ scores using TFCE with $P < .001$ uncorrected (Figure 2B and C and the Supplement [eTable 2]). Note that the correlation was driven by both male and female patients with FXS. A few voxels in the cerebellum were significantly negatively correlated with IQ scores using TFCE with $P < .001$ uncorrected (Supplement [eTable 3]). Correlations with age and the SCQ total score were not significant. All fALFF analyses included voxelwise gray matter regression so that results are independent of regional differences in gray matter density.

Figure 1. Gray Matter Density Differences Between Controls and Patients With FXS Using Voxel-Based Morphometry

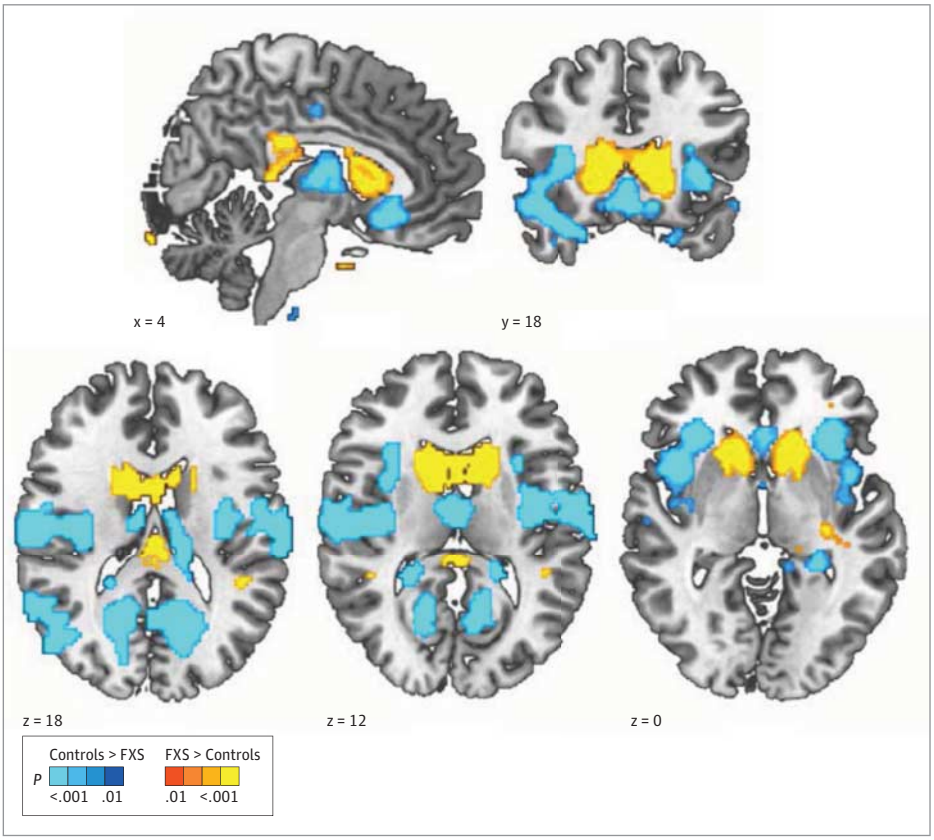

All results were obtained with the use of threshold-free cluster enhancement with $q < 0.05$, false discovery rate corrected. Red-yellow indicates regions of significantly greater gray matter density in patients with fragile X syndrome (FXS) compared with controls, and blue regions show the opposite comparison. Images are displayed in radiologic convention: the left side of the image corresponds to the right side of the brain. Coordinates refer to the x, y, and z dimensions of Montreal Neurological Institute space.

Group-Independent Component Analysis

To measure functional connectivity, the resting-state fMRI data were analyzed using the dual-regression approach. A first step in this approach is to create group-specific networks of interest using group-independent component analysis. A total of 11 networks were identified: dorsal and ventral default mode, left and right executive control, language, precuneus, salience, visuospatial, motor, primary visual, and higher visual networks (**Figure 3**A). To assess potential group differences in network connectivity, all 11 networks were included in group-level analyses.

Differences in Functional Connectivity Between FXS and Control Groups

Results showed significantly decreased functional connectivity in patients with FXS compared with controls in 5 networks: the left insular cortex within the salience network; precuneus cortex and bilateral angular gyrus within the precuneus network; left inferior frontal gyrus, left middle temporal gyrus, left superior lateral occipital gyrus, right frontal pole, and right cerebellum in the left executive control network; right middle temporal gyrus, left posterior supramarginal gyrus, and right anterior superior temporal gyrus in the language network; and left anterior supramarginal gyrus within the visuospatial network (Figure 3B and the Supplement [eTable 3]). For the opposite comparison, only the left thalamus in the primary visual network showed increased functional connectivity in patients with FXS compared with controls (Supplement [eTable 3]). All comparisons included voxelwise gray matter regression and used TFCE with a $q < 0.05$ FDR correction. Group-independent component analysis and dual-regression results were replicated when controlling for psychoactive medication status (Supplement [eFigure]).

Convergent Findings in Gray Matter Density, fALFF, and Functional Connectivity

Finally, given that similar regions showed reductions in structural and functional measures in patients with FXS compared with controls, we explored where gray matter density, fractional amplitude, and functional connectivity findings converged. For each of the 5 networks where functional connectivity was reduced in patients with FXS, we identified clusters greater than 20 voxels where between-group voxel-based morphometry, fALFF, and functional connectivity showed a reduction in FXS using TFCE with $q < 0.05$ FDR corrected. The resulting maps revealed that only the left insular cortex from the salience network intersected with fALFF and voxel-based morphometry at this threshold (**Figure 4**).

Discussion

These results provide a first look into the large-scale brain networks potentially underlying the cognitive and behavioral symptoms of FXS, the most common known form of inherited intel-

Figure 2. Brain Regions Showing Significant Reduction in fALFF in Patients With FXS

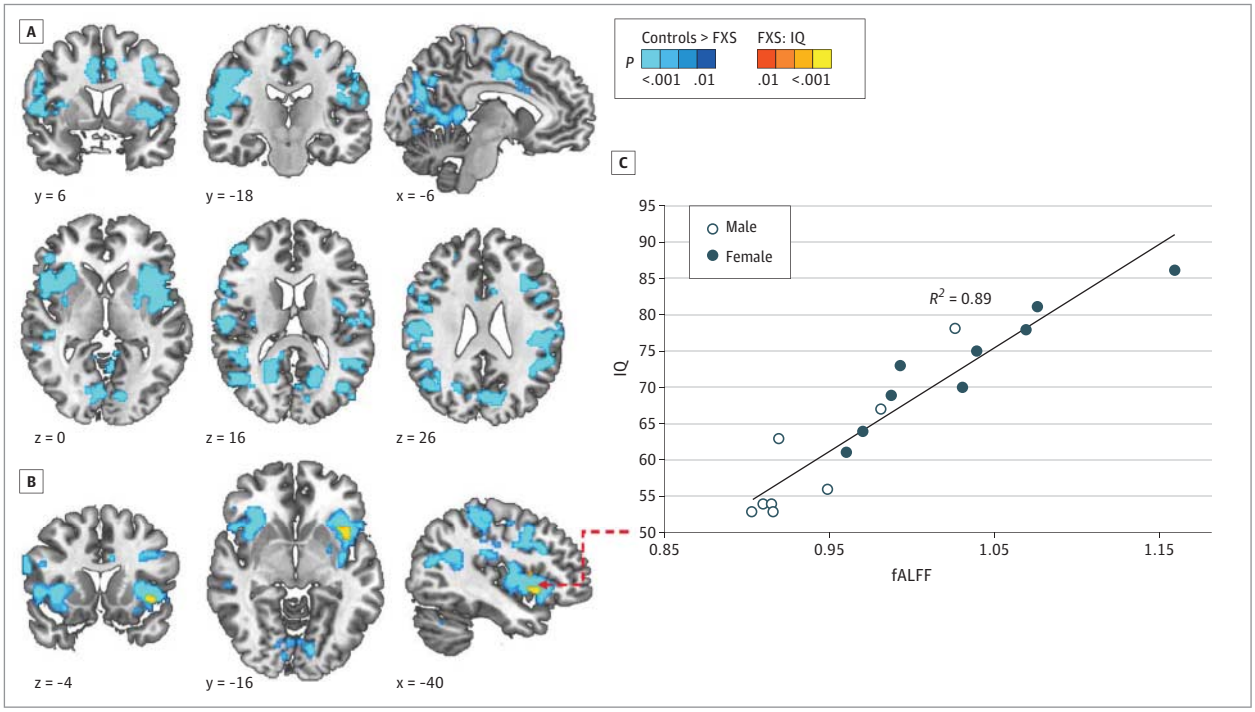

A, Analysis of fractional amplitude of low-frequency fluctuations (fALFF) between 0.01 and 0.10 Hz, using threshold-free cluster enhancement (TFCE) with $q < 0.05$ false discovery rate correction. Blue indicates areas where controls had significantly more fALFF than did patients with fragile X syndrome (FXS). No regions survived multiple comparisons correction for the opposite contrast. B, fALFF difference map for controls > FXS in blue overlaid with FXS fALFF maps positively covaried with IQ in yellow at TFCE with $P < .001$ uncorrected. A few regions in the cerebellum were negatively covaried with fALFF at TFCE with $P < .001$ (not pictured, see the Supplement [eTable 3]). C, Scatterplot of correlation between IQ scores and mean fALFF values grouped by sex within the surviving left insula cluster thresholded at $P < .001$ uncorrected. For additional details, see the Figure 1 caption.

lectual disability. Five large-scale networks were identified in which patients with FXS showed significantly decreased functional connectivity compared with matched-symptom controls: the salience, precuneus, left executive control, language, and visuospatial networks. The salience network is thought to play a role in recruiting brain regions for sensory information processing; the precuneus is involved in self-referential processing, imagery, and memory and is suggested to be a core node or hub of the default mode network. Reduced connectivity in these networks appears to map directly onto the cognitive and behavioral deficits commonly observed in individuals with FXS, including weaknesses in executive function skills, visuospatial skills, and language skills. Decreased functional connectivity in the salience network is particularly interesting given that the anterior insula, which is an important part of this network, has been suggested to play an important role in initiating dynamic switches between the executive control network and the default mode network in individuals with ASD.[7,39] In the present study, we provide evidence that the insular cortex also may be implicated in FXS. The insula is thought to be involved in a variety of functions, including interoception, as well as affective and empathic processes.[40] If the integrity of the salience network is compromised in FXS, this could explain several behavioral features in FXS, including abnormal and exaggerated autonomic responses to sensory stimulation, eye gaze aversion, and difficulties in task switching and attention.

To examine the extent to which the amplitude of low-frequency fluctuations within a region were abnormal compared with the entire spectrum, we used fALFF, a relatively new resting-state fMRI method.[21] We found that, compared with matched-symptom controls, patients with FXS showed significantly decreased fALFF in bilateral insular cortices, precuneus cortex, and anterior cingulate cortex; these regions are closely aligned to the large-scale networks identified above. We noted that fALFF in the left insular cortex was positively associated with IQ in patients with FXS. This finding does not indicate that the insula is important for IQ per se. Higher levels of fALFF in this region were found in females with FXS, and lower levels of fALLF were found in males with FXS. This result suggests that we have identified a specific biological abnormality that is correlated with sex and may contribute to (or reflect) the slowed intellectual development in children with FXS. Finally, we found that patients with FXS evidenced a neuroanatomic profile in line with previous studies (eg, increased bilateral caudate volume and reduced insula cortex volumes vs controls). These results solidify the neuroanatomic profile of region-specific differences in brain structure between patients with FXS and matched-symptom controls. Critically, the functional imaging results reported here were independent of any between-group differences in gray matter density or movement.

Many of the cognitive and behavioral features shown by individuals with FXS appear to resemble those of individuals

Figure 3. Brain Regions Showing Reduced Network Connectivity in Patients With FXS

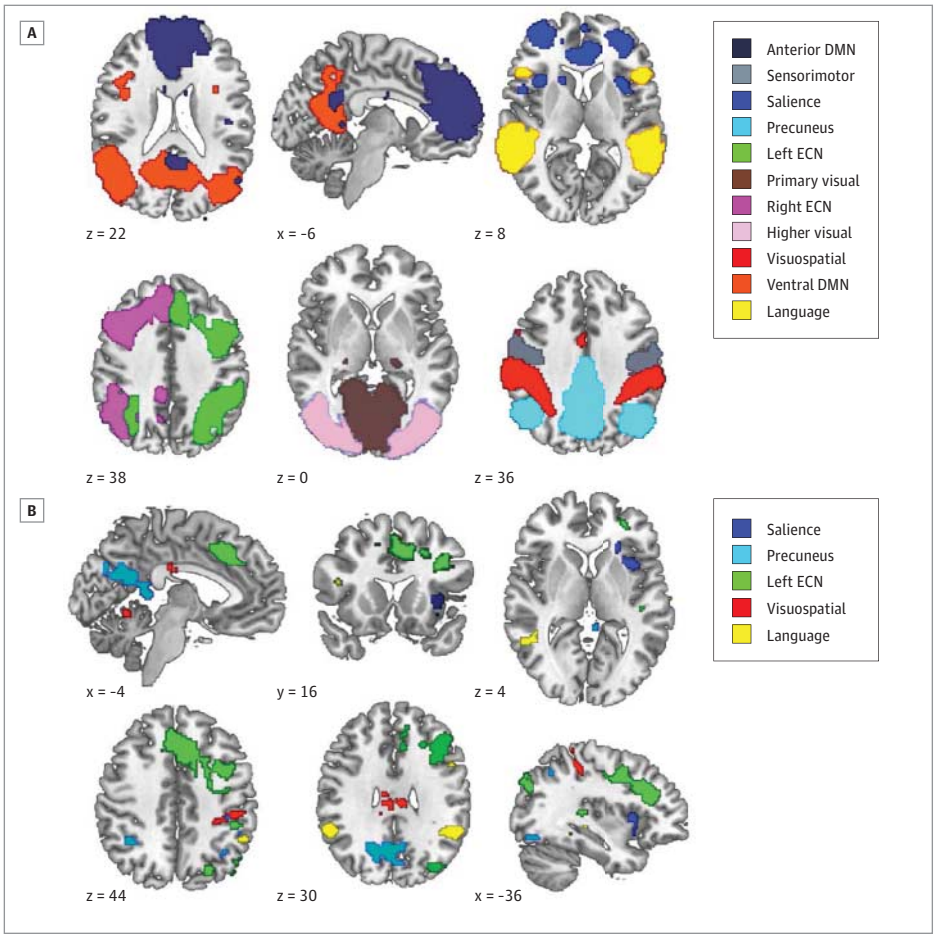

A, Group-independent component analysis depicting 11 networks coded by color: anterior and ventral default mode network (DMN), left and right executive control network (ECN), language, precuneus, salience, visuospatial, higher visual, primary visual, and sensorimotor. B, Dual regression results, controls > fragile X syndrome (FXS) using threshold-free cluster enhancement (TFCE) with $q < 0.05$ false discovery rate (FDR) corrected and color coded by network membership. One thalamic cluster in the primary visual network (not pictured) survived TFCE with $q < 0.05$ FDR correction for the opposing comparison. For additional details, see the Figure 1 caption.

Figure 4. Brain Regions Showing Reductions in Between-Group VBM, fALFF, and Functional Connectivity in Patients With FXS

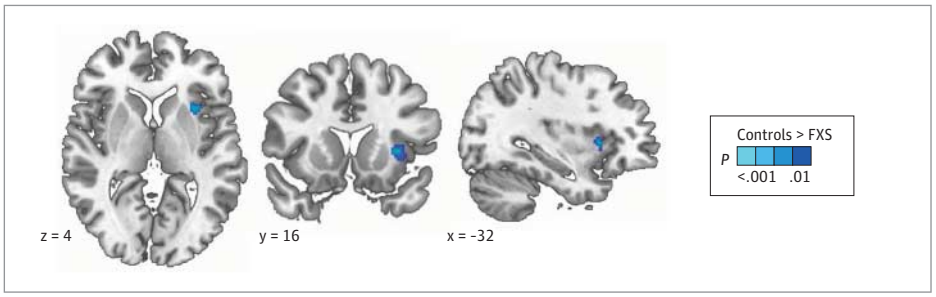

Blue region depicts surviving cluster at intersection of controls > fragile X syndrome (FXS) voxel-based morphometry (VBM), controls > FXS fractional amplitude of low-frequency fluctuations (fALFF), and controls > FXS dual regression within the salience network; threshold-free cluster enhancement with $q < 0.05$ false discovery rate correction used for each analysis. For additional details, see the Figure 1 caption.

with ASD, and several investigators[13,41] have therefore suggested that there may be behavioral and neural commonalities between the 2 disorders. Closer inspection of the items that make up the diagnostic tests for ASD appears to show that in fact there are significant behavioral differences between the 2 conditions.[13,41] Recent findings from structural and functional neuroimaging studies also appear to corroborate this position. For example, it appears that the neuroanatomic profile in FXS diverges significantly from the profile in ASD, even in early childhood (ages 1-4 years).[42] In comparison with individuals who have developmental delay but not ASD, young males with FXS were found to have decreased gray matter density in the frontal and temporal regions (including the insula), whereas males with ASD had increased gray matter density in these regions. Interestingly, the neuroanatomic profile of individuals with ASD was more similar to that in patients with developmental delay but without ASD than to those with FXS. These data further underscore the likely neurobiological heterogeneity of individuals with ASD and provide a compelling rationale for studying patients who receive a diagnosis of a well-defined neurobiological disorder, such as FXS. Indeed, it is questionable whether children with FXS can be

considered to have ASD, since FXS and ASD exist at different levels of explanation. Fragile X syndrome is an established disease, and ASD is a *DSM*-based behavioral classification. For example, members of our group have argued that conjoining FXS and ASD is tantamount to committing a "category mistake."[13] Still, the fact that our imaging data are consistent with findings in the ASD literature is intriguing, particularly given that FMRP is now known to control many genes associated with ASD and synaptic plasticity.

In neurodevelopmental research of this kind, careful consideration should be given not only to ensuring the homogeneity of the target group of interest but also to the choice of an appropriate contrast group.[43,44] Given that FXS is an X-linked neurobiological disorder, investigators have struggled to identify an appropriate contrast group to control for the putative widespread neural effects of having a significant developmental disorder, as well as the heterogeneous cognitive and behavioral symptoms typically present in FXS. Previous studies[19,42] have included groups of individuals with specific categorical diagnoses (eg, neurotypical, ASD, and developmental disability without ASD), but each of these groups fails to account for the continuum of symptom severity in FXS. We considered including a typically developing control group to examine potential differences in the average population. However, because these participants would not be matched on cognitive and behavioral symptoms, any differences between typically developing individuals and patients with FXS could simply be related to those factors. Therefore, in the present study, we used a matching strategy to ensure that individuals with FXS were well matched to those without FXS in chronological age, developmental age, and the severity of autistic and behavioral symptoms regardless of whether they also held a categorical diagnosis of ASD or developmental disability without ASD. Thus, any differences between individuals with FXS and controls would not simply be the result of differences in symptoms between the groups.

In summary, our findings demonstrate a unique, widespread neural profile present in patients with FXS compared with controls without FXS matched for age, IQ, and symptom severity. Although patients with FXS generally showed diffuse reductions in functional connectivity, converging functional and structural abnormalities in the left insular cortex, a region also suggested to underlie abnormalities in individuals diagnosed with ASD, indicates that aberrant connectivity in this region may provide researchers with a reliable, sensitive, and valid imaging biomarker for FXS. Recent studies have shown that FMRP may be involved in regulating translation and/or signaling pathways associated with many key brain systems, such as those involving glutamate,[45] acetylcholine,[46] dopamine,[47] and γ-aminobutyric acid.[48] Evidence also suggests that these neurotransmitter systems may be responsible for driving the default mode network and other large-scale brain networks at rest.[49] An important question therefore arises: Could pharmacologic agents targeted to the downstream neural systems related to reduced or absent FMRP help to normalize resting-state connectivity and, by extension, cognition and behavior in FXS? To date, only limited improvements in cognitive and behavioral functioning in FXS have been demonstrated[14] following administration of various pharmacologic agents directed to selected downstream systems. These medications include fenobam (a metabotropic glutamate receptor 5 inhibitor available for research in the United States), donepezil hydrochloride (an acetylcholinesterase inhibitor), and STX209 (a γ-aminobutyric acid B receptor agonist; also known as arbaclofen).[50] Part of the problem concerns the dearth of reliable, valid, and sensitive outcome measures available to evaluate treatment efficacy in patients with serious developmental disorders, such as FXS,[51] because many patients with this disorder are unable to complete tests that involve significant cognitive demands. Fortunately, resting-state fMRI has good test-retest reliability[52,53] and places minimal demands on the patient, requiring only that the patient remain as still as possible and awake. In the present study, we were able to obtain valid scans for 17 patients with FXS (85% of the sample) and 16 controls (80% of the sample). However, with improved methods of training the patient to remain as still as possible, as well as improved motion correction methods applied during acquisition and/or analysis, it should be possible to use resting-state fMRI to track treatment response in ongoing clinical trials for patients with FXS. We aim to establish the sensitivity and specificity of this imaging biomarker in future studies for the evaluation of pharmacologic and/or behavioral interventions in FXS.

ARTICLE INFORMATION

Submitted for Publication: August 20, 2012; final revision received January 28, 2013; accepted February 1, 2013.

Author Contributions: Ms Jiang and Dr Greicius had full access to all the data in the study and take responsibility for the integrity of the data and the accuracy of the data analysis.

Published Online: September 25, 2013. doi:10.1001/jamapsychiatry.2013.247.

Study concept and design: Hall, Reiss, Greicius.
Acquisition of data: Hall, Reiss.
Analysis and interpretation of data: All authors.
Drafting of the manuscript: Hall, Jiang, Greicius.
Critical revision of the manuscript for important intellectual content: Hall, Jiang, Reiss.
Statistical analysis: Jiang, Greicius.
Obtained funding: Hall, Reiss.
Administrative, technical, and material support: Hall, Reiss.

Conflict of Interest Disclosures: None reported.

Funding/Support: This study was funded by grants K08MH081998 (Dr Hall), MH064708 (Dr Reiss), and NS073498 (Dr Greicius) from the National Institutes of Health.

Role of the Sponsor: The National Institutes of Health had no role in the design and conduct of the study; collection, management, analysis, and interpretation of the data; and preparation, review, or approval of the manuscript; and decision to submit the manuscript for publication.

Additional Contributions: Melissa Hirt, MA; Ryan Kelley, BS; Kristin Hustyi, MA; and Jennifer Hammond, PhD, provided assistance with recruitment and scanning. Joachim Hallmayer, MD, assisted with genetic screening. All were on staff or were faculty at Stanford during the project and received salary support but no additional financial compensation for their services.

REFERENCES

1. Fox MD, Raichle ME. Spontaneous fluctuations in brain activity observed with functional magnetic resonance imaging. *Nat Rev Neurosci*. 2007;8(9):700-711.

2. Seeley WW, Menon V, Schatzberg AF, et al. Dissociable intrinsic connectivity networks for salience processing and executive control. *J Neurosci*. 2007;27(9):2349-2356.

3. Greicius MD, Flores BH, Menon V, et al. Resting-state functional connectivity in major depression: abnormally increased contributions from subgenual cingulate cortex and thalamus. *Biol Psychiatry*. 2007;62(5):429-437.

4. Greicius MD, Srivastava G, Reiss AL, Menon V. Default-mode network activity distinguishes Alzheimer's disease from healthy aging: evidence from functional MRI. *Proc Natl Acad Sci U S A*. 2004;101(13):4637-4642.

5. Damoiseaux JS, Prater KE, Miller BL, Greicius MD. Functional connectivity tracks clinical deterioration in Alzheimer's disease. *Neurobiol Aging*. 2012;33(4):828.e19-828.e30. doi:10.1016/j.neurobiolaging.2011.06.024.

6. Anderson JS, Nielsen JA, Froehlich AL, et al. Functional connectivity magnetic resonance imaging classification of autism. *Brain*. 2011;134 (pt 12):3742-3754.

7. Uddin LQ, Menon V. The anterior insula in autism: under-connected and under-examined. *Neurosci Biobehav Rev*. 2009;33(8):1198-1203.

8. von dem Hagen EA, Stoyanova RS, Baron-Cohen S, Calder AJ. Reduced functional connectivity within and between "social" resting state networks in autism spectrum conditions. *Soc Cogn Affect Neurosci*. 2012;33(8):1198-1203.

9. Just MA, Cherkassky VL, Keller TA, Kana RK, Minshew NJ. Functional and anatomical cortical underconnectivity in autism: evidence from an fMRI study of an executive function task and corpus callosum morphometry. *Cereb Cortex*. 2007;17(4):951-961.

10. Happé F, Ronald A, Plomin R. Time to give up on a single explanation for autism. *Nat Neurosci*. 2006;9(10):1218-1220.

11. Reiss AL. Childhood developmental disorders: an academic and clinical convergence point for psychiatry, neurology, psychology and pediatrics. *J Child Psychol Psychiatry*. 2009;50(1-2):87-98.

12. Harris JC. Autism spectrum diagnoses in neurogenetic syndromes: phenocopies of autism? In: Hollander E, Kolevzon A, Coyle JT, eds. *Textbook of Autism Spectrum Disorders*. Washington, DC: American Psychiatric Publishing; 2011:223-237.

13. Hall SS, Lightbody AA, Hirt M, Rezvani A, Reiss AL. Autism in fragile X syndrome: a category mistake? *J Am Acad Child Adolesc Psychiatry*. 2010;49(9):921-933.

14. Hall SS. Treatments for fragile X syndrome: a closer look at the data. *Dev Disabil Res Rev*. 2009;15(4):353-360.

15. Hessl D, Nguyen DV, Green C, et al. A solution to limitations of cognitive testing in children with intellectual disabilities: the case of fragile X syndrome. *J Neurodev Disord*. 2009;1(1):33-45.

16. Verkerk AJ, Pieretti M, Sutcliffe JS, et al. Identification of a gene (*FMR-1*) containing a CGG repeat coincident with a breakpoint cluster region exhibiting length variation in fragile X syndrome. *Cell*. 1991;65(5):905-914.

17. Greenough WT, Klintsova AY, Irwin SA, Galvez R, Bates KE, Weiler IJ. Synaptic regulation of protein synthesis and the fragile X protein. *Proc Natl Acad Sci U S A*. 2001;98(13):7101-7106.

18. Gothelf D, Furfaro JA, Hoeft F, et al. Neuroanatomy of fragile X syndrome is associated with aberrant behavior and the fragile X mental retardation protein (FMRP). *Ann Neurol*. 2008;63(1):40-51.

19. Hoeft F, Carter JC, Lightbody AA, Cody Hazlett H, Piven J, Reiss AL. Region-specific alterations in brain development in one- to three-year-old boys with fragile X syndrome. *Proc Natl Acad Sci U S A*. 2010;107(20):9335-9339.

20. Lightbody AA, Reiss AL. Gene, brain, and behavior relationships in fragile X syndrome: evidence from neuroimaging studies. *Dev Disabil Res Rev*. 2009;15(4):343-352.

21. Zou QH, Zhu CZ, Yang Y, et al. An improved approach to detection of amplitude of low-frequency fluctuation (ALFF) for resting-state fMRI: fractional ALFF. *J Neurosci Methods*. 2008;172(1):137-141.

22. Wechsler D. *The Wechsler Abbreviated Scale of Intelligence*. San Antonio, TX: Psychological Corporation; 1999.

23. Rutter M, Bailey A, Lord C. *The Social Communication Questionnaire: Manual*. Los Angeles, CA: Western Psychological Services; 2003.

24. Aman MG, Singh NN. *Aberrant Behavior Checklist: Manual*. East Aurora, NY: Slossen; 1986.

25. Glover GH, Law CS. Spiral-in/out BOLD fMRI for increased SNR and reduced susceptibility artifacts. *Magn Reson Med*. 2001;46(3):515-522.

26. Kim DH, Adalsteinsson E, Glover GH, Spielman DM. Regularized higher-order in vivo shimming. *Magn Reson Med*. 2002;48(4):715-722.

27. Smith SM, Jenkinson M, Woolrich MW, et al. Advances in functional and structural MR image analysis and implementation as FSL. *Neuroimage*. 2004;23(suppl 1):S208-S219.

28. Ashburner J, Friston KJ. Voxel-based morphometry—the methods. *Neuroimage*. 2000;11(6, pt 1):805-821.

29. Good CD, Johnsrude IS, Ashburner J, Henson RN, Friston KJ, Frackowiak RS. A voxel-based morphometric study of ageing in 465 normal adult human brains. *Neuroimage*. 2001;14(1, pt 1):21-36.

30. Smith SM. Fast robust automated brain extraction. *Hum Brain Mapp*. 2002;17(3):143-155.

31. Zhang Y, Brady M, Smith S. Segmentation of brain MR images through a hidden Markov random field model and the expectation-maximization algorithm. *IEEE Trans Med Imaging*. 2001;20(1):45-57.

32. Jenkinson M, Bannister P, Brady M, Smith S. Improved optimization for the robust and accurate linear registration and motion correction of brain images. *Neuroimage*. 2002;17(2):825-841.

33. Andersson JLR, Jenkinson M, Smith S. Non-linear registration, aka spatial normalization: 2007: FMRIB technical report TR07JA2. www.fmrib.ox.ac.uk/analysis/techrep. Published June 28, 2007. Accessed March 1, 2012.

34. Smith SM, Nichols TE. Threshold-free cluster enhancement: addressing problems of smoothing, threshold dependence and localisation in cluster inference. *Neuroimage*. 2009;44(1):83-98.

35. Song XW, Dong ZY, Long XY, et al. REST: a toolkit for resting-state functional magnetic resonance imaging data processing. *PLoS One*. 2011;6(9):e25031. doi:10.1371 /journal.pone.0025031.

36. Damoiseaux JS, Beckmann CF, Arigita EJ, et al. Reduced resting-state brain activity in the "default network" in normal aging. *Cereb Cortex*. 2008;18(8):1856-1864.

37. Nichols TE, Holmes AP. Nonparametric permutation tests for functional neuroimaging: a primer with examples. *Hum Brain Mapp*. 2002;15(1):1-25.

38. Oakes TR, Fox AS, Johnstone T, Chung MK, Kalin N, Davidson RJ. Integrating VBM into the general linear model with voxelwise anatomical covariates. *Neuroimage*. 2007;34(2):500-508.

39. Sridharan D, Levitin DJ, Menon V. A critical role for the right fronto-insular cortex in switching between central-executive and default-mode networks. *Proc Natl Acad Sci U S A*. 2008;105(34):12569-12574.

40. Mutschler I, Wieckhorst B, Kowalevski S, et al. Functional organization of the human anterior insular cortex. *Neurosci Lett*. 2009;457(2):66-70.

41. Harris JC. Brain and behavior in fragile X syndrome and idiopathic autism. *Arch Gen Psychiatry*. 2011;68(3):230-231.

42. Hoeft F, Walter E, Lightbody AA, et al. Neuroanatomical differences in toddler boys with fragile X syndrome and idiopathic autism. *Arch Gen Psychiatry*. 2011;68(3):295-305.

43. Hodapp RM, Dykens EM. Strengthening behavioral research on genetic mental retardation syndromes. *Am J Ment Retard*. 2001;106(1):4-15.

44. Dykens EM, Hodapp RM. Three steps toward improving the measurement of behavior in behavioral phenotype research. *Child Adolesc Psychiatr Clin N Am*. 2007;16(3):617-630.

45. Antar LN, Afroz R, Dictenberg JB, Carroll RC, Bassell GJ. Metabotropic glutamate receptor activation regulates fragile X mental retardation protein and *Fmr1* mRNA localization differentially in dendrites and at synapses. *J Neurosci*. 2004;24(11):2648-2655.

46. Chang S, Bray SM, Li Z, et al. Identification of small molecules rescuing fragile X syndrome phenotypes in *Drosophila*. *Nat Chem Biol*. 2008;4(4):256-263.

47. Wang H, Wu LJ, Kim SS, et al. FMRP acts as a key messenger for dopamine modulation in the forebrain. *Neuron*. 2008;59(4):634-647.

48. Olmos-Serrano JL, Paluszkiewicz SM, Martin BS, Kaufmann WE, Corbin JG, Huntsman MM. Defective GABAergic neurotransmission and pharmacological rescue of neuronal hyperexcitability in the amygdala in a mouse model of fragile X syndrome. *J Neurosci*. 2010;30(29):9929-9938.

49. Hahn A, Wadsak W, Windischberger C, et al. Differential modulation of the default mode network via serotonin-1A receptors. *Proc Natl Acad Sci U S A*. 2012;109(7):2619-2624.

50. Berry-Kravis E, Knox A, Hervey C. Targeted treatments for fragile X syndrome. *J Neurodev Disord*. 2011;3(3):193-210.

51. Hall SS, Hammond JL, Hirt M, Reiss ALA. A "learning platform" approach to outcome measurement in fragile X syndrome: a preliminary psychometric study. *J Intellect Disabil Res*. 2012;56(10):947-960.

52. Shehzad Z, Kelly AM, Reiss PT, et al. The resting brain: unconstrained yet reliable. *Cereb Cortex*. 2009;19(10):2209-2229.

53. Thomason ME, Dennis EL, Joshi AA, et al. Resting-state fMRI can reliably map neural networks in children. *Neuroimage*. 2011;55(1):165-175.